31st Annual International Conference of the IEEE EMBS
Minneapolis, Minnesota, USA, September 2-6, 2009

Multi-structure Whole Brain Registration and Population Average

Ali R. Khan and Mirza Faisal Beg

Abstract— **We present here a novel method for whole brain magnetic resonance (MR) image registration that explicitly penalizes the mismatch of cortical and subcortical regions by simultaneously utilizing anatomic segmentation information from multiple cortical and subcortical structures, represented as volumetric images, with given T1-weighted MR image for registration. The registration is computed via variational optimization in the space of smooth velocity fields in the large deformation diffeomorphic metric matching (LDDMM) framework. We tested our method using a set of 10 manually labeled brains, and found quantitatively that subcortical and cortical alignment is improved over traditional single-channel MRI registration. We use this new method to generate a volumetric and cortical surface-based population average. The average grayscale image is found to be crisp, and allows the reconstruction and labeling of the cortical surface.**

I. INTRODUCTION

Whole brain image registration is a useful tool for studying anatomical variability and pooling information into a template space. Inter-subject whole brain magnetic resonance (MR) image registration is a challenging problem because of the high degree of anatomical variability, especially in the highly convoluted folding of the cortical regions, and the size and shape of subcortical structures and ventricles. Previous approaches can be categorized into those that drive the registration using image intensity information, such as [1], [2], [3], [4], [5], [6], [7], and those that use features derived from the images, such as [8], [9]. Feature-based methods have the advantage of working with a lower dimensionality representation of the anatomy, but possibly lack information present in the original images that was not detected as features, weak edges for example.

Recent approaches have used a combination of intensity- and feature-based methods, such as [10], which computed a cortical surface registration using sulcal landmarks, extended the registration to the entire volume, followed by intensity-based refinement. Our previous work [11] used Freesurfer [12], [13] segmentations of the region of interest to provide an initial mapping for the subsequent matching using grayscale image intensities for computing a refined segmentation. A recent paper [14] compared a few approaches for registration, and showed that initialization of registration of grayscale MR images with anatomical segmentations of regions of interest outperforms the direct grayscale MR image based registration alone because of the benefit of a-priori information available on the anatomical region to be aligned. In the small deformation setting, manually identified landmarks were used to initialize registration [9] followed by multi-channel segmentation using a few semi-automatically defined subcortical structures such as caudate, putamen, thalamus and cerebellar lobes.

Existing approaches reviewed above are specialized to registering certain areas of the brain, such as subcortical or cerebellar regions [9], [10], or may employ semi-automated steps [9]. Additionally, the standard registration cost based on grayscale image overlap does not model the cost of mismatch of small and thin cortical regions, or smaller subcortical structures and can thereby be prone to local minima [14]. We propose here a novel algorithm that is completely automated, can accomodate large deformations, and by explicitly incorporating a cost term that penalizes mismatch of cortical and subcortical ROIs, designed to peform good registration at both the cortical and the subcortical ROI level, in general the whole brain level. To achieve this, we extend our LDDMM setting, shown to accomodate large variability [3], to use the automatically obtained segmentations of subcortical and cortical segmentations as "feature channels" simultaneously with the grayscale MR image to ensure robustness to matching structures over the whole brain.

In this paper we will describe our novel multi-structure LDDMM brain registration framework. We will compare the performance of using multi-structure cortical+subcortical constraints with the standard grayscale MR image registration alone using our own single channel LDDMM, and another strong frequently-used registration method. To highlight the advantage of using our multi-structure framework for whole brain registration, we show a novel application for creating a whole brain population average that is found to be sharp, and can be processed with tools such as Freesurfer for cortical parcellation.

II. METHODS

A. INITIAL BRAIN SEGMENTATION

To perform an initial automated segmentation of the whole brain, we use the Freesurfer image analysis suite, which consists of sub-cortical [15] and cortical surface [12], [13] processing streams; the former labels 37 volumetric structures, and the latter labels 68 regions of the cortical surface (including left and right distinctions).

Each brain MR image A^{MR} is represented as a function $A : \Omega \rightarrow \mathbb{R}$, where $\Omega \subseteq \mathbb{R}^3$ is the domain of the 3D MR image. Each brain was segmented into N labels, represented similarly as label images $A^{Seg,i}, i \in [1, \ldots, N]$. Note that the cortical surface parcellations were voxelized to produce volumetric cortical segmentations.

Ali R. Khan and Mirza Faisal Beg are with School of Engineering Science, Faculty of Applied Science, Simon Fraser University, 8888 University Dr, Burnaby, BC, Canada akhanf@sfu.ca, mfbeg@ensc.sfu.ca

978-1-4244-3296-7/09/$25.00 ©2009 IEEE

B. MULTI-STRUCTURE REGISTRATION

Diffeomorphic registration, that is, algorithms which ensure the resulting transformations are one to one, invertible and smooth, are desired in many medical registration applications because they preserve the topological properties of the underlying anatomy [3]. To explicitly incorporate a penalty for mismatch of labeled ROIs, we extended the existing single channel LDDMM [5] cost toward a multi-structure cost.

Let the pair A^{MR} and B^{MR} of whole brain MR images be given, and let their N segmentations, $A^{Seg,i}, i \in [1,\ldots,N]$ and $B^{Seg,i}, i \in [1,\ldots,N]$ be available. The diffeomorphic transformation matching A and B is given by $\varphi : \Omega \rightarrow \Omega$ such that $A \circ \varphi^{-1} \approx B$. This transformation φ is built from the flow of smooth time-dependent velocity vector field, $v_t \in V, t \in [0,1]$ where V is a Hilbert space of smooth, compactly supported vector fields on Ω. Such a velocity vector field defines the evolution of a curve $\phi_{0,t}, t \in [0,1]$ via the evolution equation $\dot{\phi}_{0,t} = v_t(\phi_{0,t})$ such that the end point $\phi_{0,1}$ of the curve ϕ at time $t = 1$ is the particular transformation $\varphi = \phi_{0,1}$ that is sought for registration. Let the notation $\phi_{s,t} : \Omega \rightarrow \Omega$ denote the composition $\phi_{s,t} = \phi_t \circ (\phi_s)^{-1}$ with the interpretation that $\phi_{s,t}(y)$ is the position at time t of a particle that is at position y at time s. Hence, the transformed image A is given by $A \circ \varphi^{-1} = A \circ \phi_{1,0} \approx B$ and the transformed target image is $B \circ \phi_{0,1}$. The energy functional for our multi-channel registration is:

$$E(v) = \int_0^1 \|v_t\|_V^2 \mathrm{d}t + \lambda^{MR}\|A^{MR} \circ \phi_{1,0} - B^{MR}\|_{L^2}^2 + \sum_{i=1}^{N} \lambda^{Seg,i}\|A^{Seg,i} \circ \phi_{1,0} - B^{Seg,i}\|_{L^2}^2, \quad (1)$$

We discretized the derived gradient and used a simple update scheme, $v_t^{r+1} = v_t^r - \epsilon\nabla_v E_t$, to get the updated velocity field at iteration r given the previous iteration. Details of the numerical implementation and algorithm can be seen in [5]. The software implementation is in C++ and uses the Message Passing Interface (MPI) for parallelization.

C. POPULATION AVERAGE CONSTRUCTION

We extended the unbiased diffeomorphic atlas construction method described in [16] to incorporate multi-structure registration. The new multi-structure cost for computing the population average grayscale image, defined as the image $\bar{I}$ that has minimal distance to each image in the database, is extended from the single channel [16] version to give :

$$\{\bar{\varphi}_i, \bar{I}\} = \underset{\varphi_i \in \mathcal{G}, I \in \mathcal{I}}{\operatorname{argmin}} \sum_{j=1}^{M} \Bigg(\int_0^1 \|v_t^j\|_V^2 \mathrm{d}t + \lambda^{MR}\|I^{MR} \circ \varphi_i - I_j^{MR}\|_{L^2}^2 + \sum_{i=1}^{N} \lambda^{Seg,i}\|I^{Seg,i} \circ \phi_{1,0} - I_j^{Seg,i}\|_{L^2}^2 \Bigg), \quad (2)$$

For fixed transformations φ_i, the average image is:

$$\bar{I} = (1/M)\sum_{j=1}^{M} \frac{|D\varphi_j|}{\sum_{k=1}^{M}|D\varphi_k|} I_j \circ \varphi_j, \quad (3)$$

where $\bar{I}$ is a multi-channel image consisting of $\bar{I}^{MR}$ and N segmentation channels, $\bar{I}^{Seg,i}$. We optimize the cost using an iterative algorithm:

Input: Set of images $I_1, I_2, \ldots, I_M$
Output: Ensemble average Image $\bar{I}$
Set iteration number n = 0, $v_t^{j(n)} = 0$, $\varphi_j^{(n)}$ = id ;
while $\sum_{j=1}^{M}\int_0^1 \|v_t^{j(n+1)}\|_V^2 \mathrm{d}t < \sum_{j=1}^{M}\int_0^1 \|v_t^{j(n)}\|_V^2 \mathrm{d}t$ **do**
  $\bar{I}^{(n)}(x) = (1/M)\sum_{j=1}^{M} \frac{|D\varphi_j^{(n)}(x)|}{\sum_{k=1}^{M}|D\varphi_j^{(n)}(x)|} I_j \circ \varphi_j^{(n)}(x)$;;
  foreach I_i **do**
    while *Optimum not found* **do**
      Compute gradient for multi-structure LDDMM cost (equation 1), $\nabla_{v^{j(n)}} E(v^{j(n)})$ for matching $\bar{I}^{(n)}$ to I_j;
      Compute new velocity $v_t^{j(n+1)} = v_t^{j(n)} - \epsilon\nabla_{v^{j(n)}} E(v^{j(n)})$;
    end
  end
end

Algorithm 1: Multi-structure unbiased LDDMM average

Upon generation of the population average brain image, $\bar{I}^{MR}$, we then used Freesurfer's cortical reconstruction on the average volume to create a population average cortical surface. Thus, the end result is a volumetric and cortical surface-based population average consisting of an average MR image and it's corresponding cortical surface.

D. EXPERIMENTS

We carried out inter-subject brain registration experiments to test the performance of single channel LDDMM registration (MR image only), and multi-structure LDDMM registration (MR images with subcortical and cortical constraints). We chose not to skull strip the images since any inconsistencies in the automated skull stripping could cause mapping errors in the registration as left-over skull could be mapped to the brain or vice versa.

For each hemisphere, we used a subset of the subcortical structures consisting of: lateral ventricle, caudate nucleus, putamen, pallidum, nucleus accumbens, thalamus, hippocampus and amygdala, and we used all 34 cortical region labels, as listed in [12]. We smoothed the binary segmentations with a Gaussian neighbourhood filter ($\sigma = 2$) to eliminate the sharp boundaries present.

We ran this registration algorithm for 256x256x128 whole brain images with Dell R900 compute servers having 12x3.6 GHz Xeon processors and 128 GB of memory.

For comparison to an existing brain registration method, we used IRTK [6], which uses B-spline free-form deformations and was ranked as one of the top-performing brain registration algorithms in a recent evaluation [7]. The inter-subject brain registration experiments used MR images from

the Internet Brain Segmentation Repository (IBSR), and the population average used MR scans from 10 elderly subjects.

III. RESULTS

To quantify registration accuracy, we transformed the manual segmentations and cortical surfaces of the target brain images to the template space, and compared the propagated segmentations and surfaces to the template manual segmentations and surfaces both qualitatively (visualization), and quantitatively (volumetric overlap and boundary distance errors). Volumetric overlap was measured using the Dice similarity coefficient: $DSC(A,B) = 2\frac{V(A\cap B)}{V(A)+V(B)}$ where $V(A)$ and $V(B)$ are the volumes of binary segmentations A and B. Boundary distance errors for a given pair of surfaces were measured using a symmetrized mean surface distance, $SD(A,B) = \max sd(A,B), sd(B,A)$, where $sd(A,B) = \frac{1}{N_A}\sum_{a\in A}\min_{b\in B} d(a,b)$, is the directed mean surface distance.

Figure 1 plots the volumetric overlap metrics for the manual segmentations propagated with LDDMM, Multi-structure LDDMM, and IRTK for comparison. We see here that LDDMM registration has higher overlaps for IRTK for most structures, and multi-structure LDDMM further improves these, most notably in the hippocampus and amygdala.

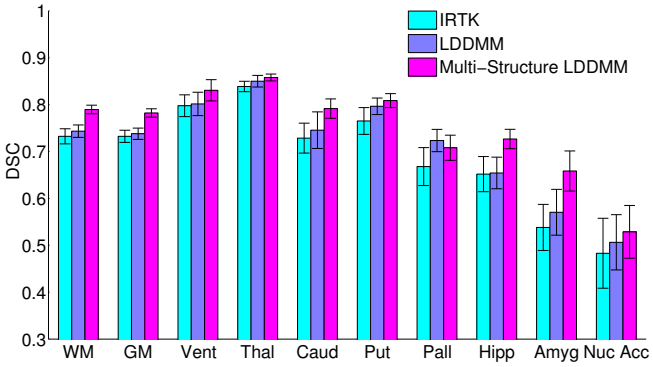

Fig. 1. Dice similarity coefficients for the propagated target manual segmentations ($IBSR_{10} - IBSR_{18}$) and the template manual segmentations, shown for single channel LDDMM registration (LDDMM), with added multi-structure constraints (Multi-structure LDDMM) and B-spline registration (IRTK). The mean of the 9 subjects is shown for each structure, with error bar height equal to the standard deviation.

For each cortical parcellation given by Freesurfer (34 different labels on each hemisphere), we computed the mean surface distance between the template cortical surface and each propagated target cortical surface. A visualization of the mean surface distances on the cortical surface of the template brain is shown in Figure 2, comparing LDDMM and multi-structure LDDMM registration; the multi-structure registration is shown to further reduce the mean surface distance in the cortex to less than 2 mm.

For a qualitative comparison of cortical registration, Figure 3 shows a representative sagittal slice of the template brain with the reference and propagated cortical surfaces outlined. Here we see a clear improvement in registration when cortical segmentation constraints are added.

Results for our multi-structure population average are shown in Figure 4, along with the population average generated using single-channel MR-only LDDMM registration. The cortical surfaces shown were reconstructed and parcellated from the average volumes using Freesurfer.

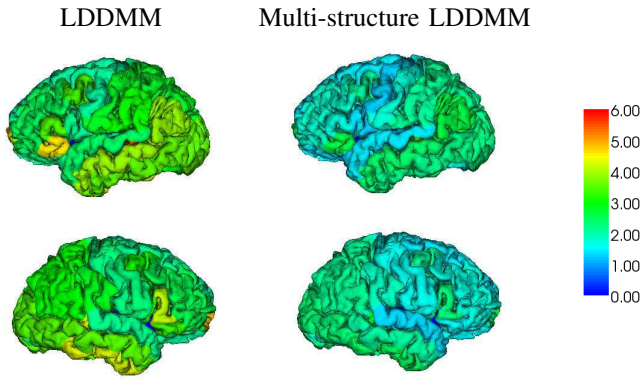

Fig. 2. Mean surface distance: Visualization of the left (top) and right (bottom) cortical surface of the template brain, with each cortical parcellation coloured with the mean surface distance (mm) in that region to it's corresponding parcellation in the transformed target brain. Single-channel LDDMM registration (left) is compared to multi-structure LDDMM registration (right).

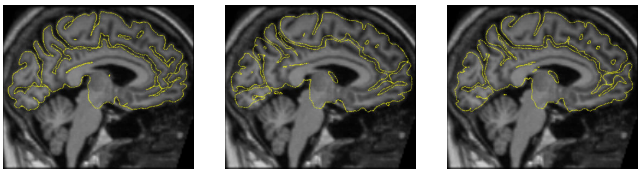

Fig. 3. Sagittal MR slices of the template brain ($IBSR_{09}$) showing cortical surface outlines generated on the template brain (Reference), and propagated from one of the target brains ($IBSR_{10}$) using single-channel (LDDMM), and Multi-structure LDDMM registration.

IV. CONCLUSIONS AND DISCUSSION

In this paper, we have presented a fully automated and novel multi-structure whole brain registration method by simultaneous matching MR grayscale images and explicitly incorporating penalty for mismatch of cortical and subcortical segmentations. The results for whole brain MR images using this multi-structure method are promising, with notable improvements in cortical as well as subcortical alignment. Application of this method to generate a population average grayscale image gives a resulting average image the exhibits the major cortical folds well enough for cortical surface reconstruction through Freesurfer.

Population averages are a valuable tool for interpretation, visualization and processing of anatomical data [16], [17], [18], [19]. It is known that the misalignment in registration leads to a blurred average brain image [20], as can be seen in the MNI305 atlas [1], which used a low dimensional transformation model for normalization, and also in recent

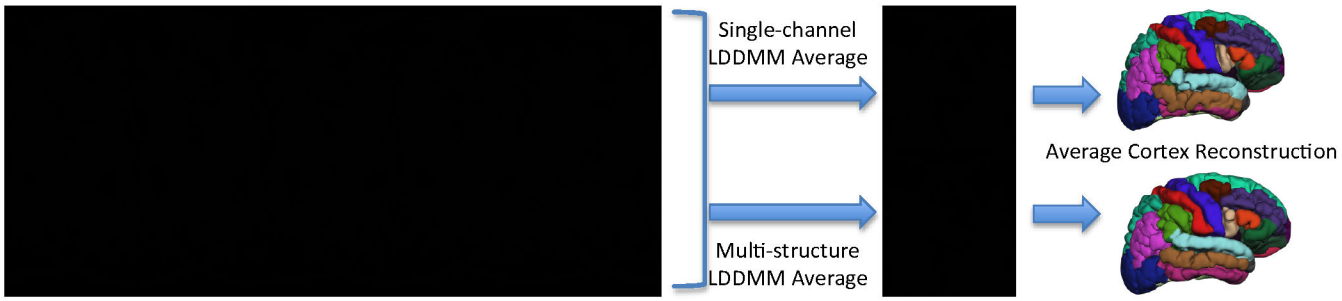

Fig. 4. The 10 elderly subjects used in the population average and the average images generated using single channel (MR only) LDDMM, and multi-structure LDDMM. Average volumes were run through Freesurfer's cortical reconstruction and parcellation, with the right hemisphere shown.

work aimed at the construction of cortical atlases [19]. Our population average exhibits many prominent and sharp cortical features, likely due to the high-dimensional transformation (LDDMM) and the multi-structure constraints which help overcome local minima and aid alignment. We demonstrated the quality of our volumetric population averages by performing standard cortical reconstruction and parcellation; the generated cortical surface remarkably displays the major cortical sulci and gyri with an accuracy not seen before with volumetric-based methods alone.

One issue that merits further consideration is that the weights of individual channels (the λ in Eq. 1) need to be chosen, and at this time are fixed to be equal. However, these could be optimized over a small training database for best whole brain registration in a principled way. Another approach would be to weight the relative channel contributions of the segmentation channels to be inversely proportional to the size of the structures, so errors in alignment over smaller structures are penalized more heavily.

Our multi-structure framework has the significant advantage of being flexible enough to allow use of computed features derived from grayscale or multi-modality images (such as edge map images, eigenvectors or fractional anisotropy maps) if available. It can also directly incorporate the simultaneous matching of internal landmarks and available cortical surfaces, in addition to matching the volumetric representation of the cortical mantle. One potential downside associated with this method is it's computational cost. The multi-structure registration using subcortical and cortical constraints took an average of 16.8 hours using 8 processors. However, thanks to significantly increasing hardware capabilities in face of rapidly decreasing hardware costs, and to initiatives such as the Bioinformatics research network (BIRN), the tradeoff between computational cost and enhanced accuracy of the whole brain registration would likely be acceptable.

REFERENCES

[1] D. Collins, *et al.*, "Automatic 3D intersubject registration of MR volumetric data in standardized talairach space." *Journal of Computer Assisted Tomography*, Jan 1994.

[2] K. Friston, *et al.*, "Spatial registration and normalization of images," *Human Brain Mapping*, vol. 2, pp. 165–189, 1995.

[3] G. E. Christensen, S. C. Joshi, and M. I. Miller, "Volumetric transformation of brain anatomy," *IEEE Transactions on Medical Imaging*, 1997.

[4] J. P. Thirion, "Image matching as a diffusion process: an analogy with maxwell's demons," *Medical Image Analysis*, vol. 2, no. 3, pp. 243–260, 1998.

[5] M. F. Beg, *et al.*, "Computing large deformation metric mappings via geodesic flows of diffeomorphisms," *International Journal of Computer Vision*, vol. 61, no. 2, pp. 139–157, 2005.

[6] D. Rueckert, *et al.*, "Nonrigid registration using free-form deformations: application to breast MR images," *IEEE Transactions on Medical Imaging*, Jan 1999.

[7] A. Klein, *et al.*, "Evaluation of 14 nonlinear deformation algorithms applied to human brain MRI registration," *Neuroimage*, vol. In Press, Accepted Manuscript, pp. –, 2009.

[8] D. Shen and C. Davatzikos, "HAMMER: hierarchical attribute matching mechanism for elastic registration," *Medical Imaging, IEEE Transactions on*, vol. 21, no. 11, pp. 1421–1439, 2002.

[9] V. A. Magnotta, *et al.*, "Subcortical, cerebellar, and magnetic resonance based consistent brain image registration." *Neuroimage*, vol. 19, no. 2 Pt 1, pp. 233–245, Jun 2003.

[10] A. Joshi, *et al.*, "Surface-constrained volumetric brain registration using harmonic mappings," *IEEE Transactions on Medical Imaging*, vol. 26, no. 12, pp. 1657–1669, 2007.

[11] A. R. Khan, L. Wang, and M. F. Beg, "Freesurfer-initiated fully-automated subcortical brain segmentation in MRI using large deformation diffeomorphic metric mapping," *Neuroimage*, vol. 41, no. 3, pp. 735–46, Jul 2008.

[12] A. Dale, B. Fischl, and M. Sereno, "Cortical surface-based analysis: I. segmentation and surface reconstruction," *Neuroimage*, vol. 9, no. 2, pp. 179–194, 1999.

[13] B. Fischl, M. I. Sereno, and A. M. Dale, "Cortical surface-based analysis: II: Inflation, flattening, and a surface-based coordinate system," *Neuroimage*, vol. 9, no. 2, pp. 195–207, 1999.

[14] M. A. Yassa and C. E. Stark, "A quantitative evaluation of cross-participant registration techniques for MRI studies of the medial temporal lobe," *Neuroimage*, vol. 44, no. 2, pp. 319 – 327, 2009.

[15] B. Fischl, *et al.*, "Whole brain segmentation automated labeling of neuroanatomical structures in the human brain," *Neuron*, vol. 33, no. 3, pp. 341–355, 2002.

[16] S. Joshi, *et al.*, "Unbiased diffeomorphic atlas construction for computational anatomy," *Neuroimage*, Jan 2004.

[17] M. S. Mega, *et al.*, "Automated brain tissue assessment in the elderly and demented population: construction and validation of a sub-volume probabilistic brain atlas," *Neuroimage*, vol. 26, no. 4, pp. 1009–18, Jul 2005.

[18] M. F. Beg and A. R. Khan, "Computing an average anatomical atlas using LDDMM and geodesic shooting," *Biomedical Imaging: Nano to Macro, 2006. 3rd IEEE International Symposium on*, pp. 1116–1119, 2006.

[19] D. Shattuck, *et al.*, "Construction of a 3D probabilistic atlas of human cortical structures," *Neuroimage*, Jan 2008.

[20] M. Wu, *et al.*, "Quantitative comparison of AIR, SPM, and the fully deformable model for atlas-based segmentation of functional and structural MR images," *Human Brain Mapping*, vol. 27, no. 9, pp. 747–54, Sep 2006.